Catalysis Today 157 (2010) 345–350

Contents lists available at ScienceDirect

Catalysis Today

journal homepage: www.elsevier.com/locate/cattod

Catalytic oxidative cracking as a route to olefins: Oxidative conversion of hexane over MoO_3-Li/MgO

Cassia Boyadjian, Bart van der Veer, Igor V. Babich, Leon Lefferts, K. Seshan [*]

Catalytic Processes & Materials, Faculty of Science & Technology, University of Twente, IMPACT, PO Box 217, 7500 AE Enschede, The Netherlands

ARTICLE INFO

Article history:
Available online 21 February 2010

Keywords:
Oxidative cracking
Hexane
Li/MgO
MoO_3-Li/MgO

ABSTRACT

Li/MgO shows promise as catalyst for oxidative cracking of hexane. However, it suffers from low catalyst activity and slight deactivation. Aiming at higher yields of C_2–C_4 olefins during the oxidative cracking of hexane, modification of sol–gel Li/MgO with MoO_3 is reported. The influence of varying loadings of MoO_3 on performance of Li/MgO during the oxidative cracking of hexane has been studied. Catalyst with minimum MoO_3 loading (0.5 wt%) shows best yields to C_2–C_4 olefins. Promotion by MoO_3 maintains higher surface area upon calcination at $T > 500\,^{\circ}C$ and improves catalyst stability significantly by minimizing surface carbonate formation.

1. Introduction

Catalytic oxidative cracking of naphtha is conceptually an alternative process to steam cracking. Co-feeding oxygen and presence of catalyst facilitate cracking to occur at lower temperatures, thus making the overall process less energy consuming. The development of an efficient catalyst, however, remains a challenge. The right catalyst should be able to selectively activate the paraffin in the presence of the very reactive olefins, thus inhibiting the consecutive deep oxidation of the product olefins. Very little information is reported in literature regarding catalytic oxidative cracking of naphtha range hydrocarbons. From this information available, typically three classes of catalysts have been tested for catalytic cracking of naphtha range hydrocarbons; acidic catalysts (Ag-mordenite/Al_2O_3, Cu/HZSM-5, steamed HZSM-5), basic catalysts (CaO-SrO-Al_2O_3, WO_3-K_2O-Al_2O_3, KVO_3/corundum) and transition metal oxide catalysts (Cr_2O_3/Al_2O_3, V-oxides) [1]. Modification of rare earth oxide catalysts (CeO_2, Pr_6O_{11}, Tb_4O_7) by alkali metals such as Li and K minimized the CO_x formation during oxidative cracking [1]. Recently, we reported [2] on the performance of Li/MgO catalyst for the oxidative cracking of hexane. The catalyst showed reasonable activity and very good selectivity to C_2–C_4 olefins (~60 mol%) at a temperature as low as 575 °C, which is much lower than temperatures used in steam crackers ($T \geq 800\,^{\circ}C$). Similar to what is reported in literature for oxidative conversion of lower paraffins (methane, ethane, propane) [3–9], in the case of hexane we proposed hexane activation on the Li^+O^- sites of Li/MgO. The hexyl radical formed then undergoes complex radical chemistry in gas phase in presence of molecular oxygen, forming the product mixture of C_1–C_5 products, including paraffins, olefins and combustion products.

A disadvantage of the Li/MgO is that the active sites of the catalyst are susceptible for deactivation during reaction upon interaction with product CO_2. Stability test of Li/MgO catalyst during oxidative cracking of hexane showed that it suffers from partial deactivation during the first hour of time on stream [2]. This poisoning effect of CO_2 on Li^+O^- active sites of Li/MgO has been repeatedly reported in literature [5,10–11]. During the oxidative coupling of methane Lunsford and coworkers [10] reported that reaction of product CO_2 with Li^+O^- results with formation of $Li^+CO_3{}^-$ which is most likely converted into the more stable Li_2CO_3 with time. In situ FTIR spectra of Li/MgO during the oxidative coupling of methane indicated the presence of adsorbed CO_2 ($O^-{\cdot}CO_2$) in addition to the presence of stable Li_2CO_3 phase [11]. Similar observations were also made by Galuszka [12]. Li_2CO_3 is not only formed during reaction but is also an inherent property of the catalyst as a result of interaction of ambient CO_2 with Li_2O during the preparation of Li/MgO catalyst [7]. FTIR spectra of freshly prepared Li/MgO catalyst and calcined at 600 °C, showed bands attributed to presence of Li_2CO_3 in the catalyst [13].

Unlike in the case of oxidic catalysts with redox properties [6], sequential combustion of olefins over Li/MgO is less of a problem. This is due to the non red-ox nature of the catalyst and its lower oxidation capacity. Hence, olefin selectivity over Li/MgO is almost invariant with the hexane conversion levels [2]. Lower oxidation activity also implies that hexane conversions are lower. Therefore, we recently investigated the modification of Li/MgO with small amounts of red-ox promoters [2]. Our objective was to increase

---

[*] Corresponding author. Tel.: +31 53 489 3254, fax: +31 53 489 4683.
E-mail address: k.seshan@utwente.nl (K. Seshan).

0920-5861/$ – see front matter © 2010 Elsevier B.V. All rights reserved.
doi:10.1016/j.cattod.2010.01.028

catalyst activity by possibly enhancing C–H bond scission in hexane, which is the rate-limiting step. Three promoters were investigated: V_2O_5, Bi_2O_3 and MoO_3. Both MoO_3 and Bi_2O_3 resulted in considerable improvements in the yields of C_2–C_4 olefins, while V_2O_5 resulted in formation of more combustion products [2]. Promotion of Li/MgO with Bi_2O_3 and MoO_3 oxides resulted in an increase in initial hexane conversions as expected and a significant improvement in the yields of olefins. Moreover, the promoted catalysts were stable probably due to lower carbonate formation [2].

In this paper we try to understand the role of MoO_3 in improving the yields of light olefins during oxidative cracking of hexane. Our objective is to verify whether MoO_3 enhances C–H bond scission in hexane and to investigate role of MoO_3 in minimizing the concentration of surface carbonates. Optimization of MoO_3 levels is reported.

Table 1
BET and XRF data of catalysts.

Catalyst[a]	BET surface area (m^2/g)	MoO_3 (wt%)	θ (%)[c]
Li/MgO[b]	106		
0.2Mo-Li	36	0.23	5.21
0.5Mo-Li	70	0.51	6.13
3.6Mo-Li	76	3.58	41.03
7.1Mo-Li	82	7.11	78.28
MgO[b]	195		
0.5Mo-MgO	144	0.52	3.04
3.3Mo-MgO	178	3.26	15.82
7.9Mo-MgO	189	7.94	38.16

[a] Li content in all samples is ~ 0.86 wt%.
[b] Calcined at 500 °C.
[c] Theoretical surface coverage of Li/MgO by MoO_3 assuming monolayer.

2. Experimental

2.1. Materials

Commercially available $Mg(OCH_3)_2$ solution in methanol (Aldrich, 6–8 wt% in methanol), methanol (Merck) and $LiNO_3$ (Aldrich, assay ≥99.99%) were used for preparation of MgO and Li/MgO catalysts. Ammonium molybdate (Aldrich, 99.98%) was used as precursor for MoO_3. Pure hexane (Fluka, GC assay ≥99.0%) was used for catalytic experiments. MoO_3 (Aldrich, assay 99.99%) was used for TPD experiment.

2.2. Catalyst preparation

Sol–gel synthesized MgO and Li/MgO catalysts used in this study were prepared according to the method described in [7]. A methanol solution containing $Mg(OCH_3)_2$ (0.4 M) was mixed at room temperature with another methanol solution containing water (0.8 M) to form a sol. For Li/MgO the required amount of $LiNO_3$ was added to the solution to obtain ~1 wt% Li. The solution was allowed to stay for gelation for 24 h. The gel formed was dried at 50 °C in vacuum for 7 h, and calcined at 500 °C in air for 1 h. Modified MoO_3-Li/MgO catalysts were prepared by wet impregnation of the sol–gel synthesized Li/MgO using aqueous solution of the ammonium molybdate. The modified catalysts were then dried at 50 °C in vacuum for 7 h and calcined at 600 °C for 5 h with a heating rate of 5 °C/min. Under the conditions used for calcination (600 °C) ammonium molybdate completely decomposes to MoO_3. Similarly, MoO_3-MgO catalysts were prepared by the wet impregnation of the sol–gel synthesized MgO.

2.3. Sample characterization

BET surface area of the catalyst was determined with nitrogen physisorption using a Micro-metrics Tristar instrument. The samples were out-gassed in vacuum at 250 °C for 24 h prior to the analysis. X-ray diffraction patterns were recorded by a Philips PW 1830 diffractometer using Cu Kα radiation, λ = 0.1544 nm. XRD patterns were measured in reflection geometry in the 2θ range between 35° and 50°. Elemental composition of Li was determined with atomic absorption spectroscopy (AAS). MoO_3 loadings were determined with X-ray fluorescence spectroscopy (XRF, Phillips PW 1480 spectrometer). Results are presented in Table 1. MoO_3 promoted samples are denoted as *x*Mo-Li and *x*Mo-MgO, where *x* is wt% of MoO_3.

2.4. Catalytic tests

The catalytic tests were carried out at atmospheric pressure and isothermal conditions in a fixed-bed reactor. An alumina tube reactor of 4 mm internal diameter was used. The catalyst bed (10 mm length) was packed between two quartz-wool plugs in the alumina reactor. Powder catalyst was pressed, crushed and sieved to particle size of 0.4–0.6 mm before use. An alumina rod of 3 mm internal diameter was placed right below the catalytic bed to reduce the post catalytic volume in order to minimize homogenous gas phase reactions. A Chromel–Alumel thermocouple inside a quartz tube was inserted above the catalytic bed to record reaction temperature. The temperature of the furnace was controlled by a second thermocouple placed outside the reactor tube within the isothermal zone of the tubular furnace.

Reactions were studied in the temperature range between 475 and 575 °C. Feed (100 ml/min) consisted of 10 mol% of hexane vapor, 8 mol% of O_2 and balance helium. Before each catalytic test, the catalysts were pretreated in 50% O_2/He (60 ml/min) for 1 h at a temperature of 625 °C. For analysis of the product, samples were injected into two micro GCs every 5 min during a period of 5 h. A detailed description of the experimental setup is given elsewhere [2].

Hexane conversions were calculated on carbon mol basis; i.e. (C_{6in} moles − C_{6out} moles)/C_{6in} moles × 100%. The carbon balance closed between 100 and 105%. Selectivity to individual products was also calculated based on the number of moles of carbon contained in the products, divided by the total number of moles of carbon in the product mixture excluding unconverted feed; i.e. $(n_iC_i/\sum n_iC_i) \times 100\%$.

2.5. Temperature programmed desorption (TPD)

TPD experiments were performed in the same experimental setup used for testing the catalyst. 100 mg of samples were used. Three sets of TPD experiments were conducted. (i) Fresh Li/MgO and MoO_3 promoted catalysts; the fresh catalysts were pretreated in O_2/He at 600 °C for 1 h to decompose any $MgCO_3$ present. After cooling the catalysts to 100 °C in He, TPD was conducted. (ii) Li/MgO; sample was pretreated in O_2/He at 600 °C for 1 h. It was then cooled to 575 °C and exposed to 50 ml/min of 10% CO_2/He for 1 h. After purging the catalyst in He and cooling down to 100 °C, TPD was conducted. (iii) MgO and MoO_3; samples were pretreated in O_2/He at 600 °C for 1 h. They were then exposed to 50 ml/min of 10% CO_2/He and simultaneously allowed to cool down to 100 °C. After purging the samples in He, TPD was conducted. In all experiments TPD was conducted from 100 to 950 °C (except with MoO_3 from 100 to 800 °C), with an increment of 10 °C/min, with He flow of 10 ml/min as a carrier gas. The catalyst sample was allowed to stay at the final temperature for half an hour. The concentration of desorbed CO_2 was determined with the quad micro GC (PPQ column) every 2 min.

3. Results

3.1. Effect of MoO_3 on BET surface area of the catalyst

Characteristics of the catalysts used in this study are shown in Table 1. 0.5 wt% MoO_3 promoted Li/MgO maintained higher surface area (70 m^2/g) upon calcination at 600 °C, than the unpromoted one (15 m^2/g). As shown in Fig. 1, Li/MgO undergoes a dramatic decrease in surface area upon calcination at temperatures above 500 °C. This detrimental effect of temperature on surface area is not observed in the case of MgO. The effect of MoO_3 on surface area of Li/MgO was more pronounced for 0.5 wt% and higher MoO_3 loadings, as also shown in Table 1. In the presence of MoO_3 the high surface areas were retained after the high temperature heat treatment. In order to confirm the role of MoO_3 in maintaining higher surface area, we impregnated the sol-synthesized Li/MgO with water only and then calcined at 600 °C, mimicking the procedure of MoO_3 impregnation. The catalyst exhibited very low surface area (8 m^2/g).

Fig. 2 presents XRD of Li/MgO and MoO_3 promoted catalysts. All catalysts exhibited peaks attributing to MgO. XRD of Mo containing samples did not show any additional peaks to indicate formation of new crystalline phases. Hence, we assume that Mo is present as MoO_3. However, the observed shift in the peak positions in the MoO_3 containing samples compared to Li/MgO, might indicate formation of solid solutions between MoO_3 and Li-MgO support.

3.2. Temperature programmed desorption

Temperature programmed desorption was performed for Li/MgO and MoO_3 promoted Li/MgO catalysts. Fig. 3 presents results of these experiments. TPD of Li/MgO exhibited a CO_2 desorption peak at 860 °C which is typical for Li_2CO_3 [10]. The presence of Li_2CO_3 (formed with CO_2 from ambient) is an inherent property of Li/MgO [7,14]. TPD of the MoO_3 promoted catalysts exhibited similar Li_2CO_3 peak, however with lower intensity. This peak continued to decrease with increasing MoO_3 loadings. This confirms the gradual decrease in the amount of Li_2CO_3 in Li/MgO with increasing MoO_3 loadings. The small desorption peak observed at around 700 °C in both 0.2Mo-Li and 0.5Mo-Li catalysts, is attributed to desorption of adsorbed CO_2 from ambient on Li^+O^- active sites ($Li^+CO_3{}^-$) of Li/MgO. Li/MgO (see insert) also exhibited similar CO_2 desorption peak at around 650 °C. During TPD of CO_2 from Li/MgO, Lunsford and coworkers [10] attributed the CO_2 desorption peak at around 630 °C to CO_2 adsorbed on Li^+O^- sites. In the high MoO_3 loaded sample (7.1Mo-Li), this was absent indicating the influence of MoO_3 on suppressing all types of carbonates. TPD of CO_2 of MoO_3 showed no significant CO_2 desorption peak, while TPD of MgO showed a broad desorption peak ($MgCO_3$ decomposition) of CO_2 between 100 and 600 °C with a maximum at 275 °C (see the insert).

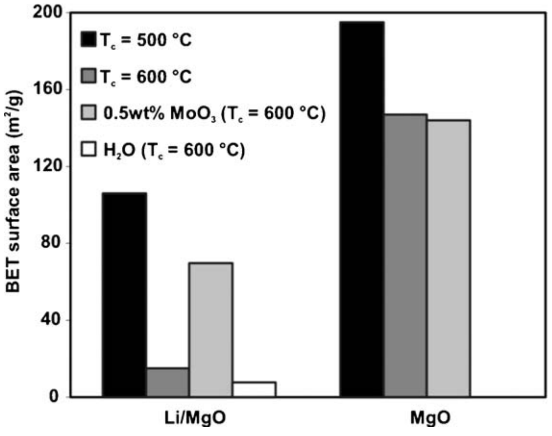

Fig. 1. BET surface area of Li/MgO and MgO at different calcination temperatures before and after promotion with MoO_3.

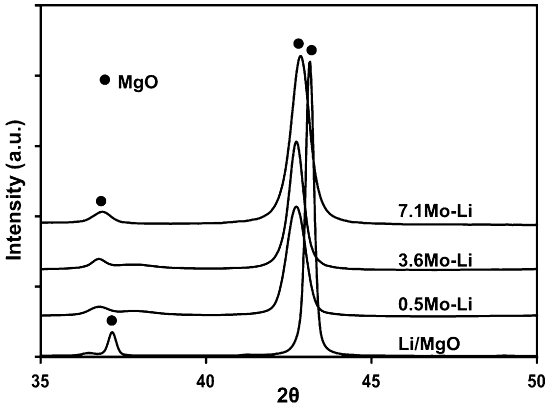

Fig. 2. XRD of Li/MgO and MoO_3-Li/MgO catalysts.

3.3. Catalytic tests

The influence of varying loadings of MoO_3 on the performance of Li/MgO during the oxidative cracking of hexane was investigated in the temperature range between 475 and 575 °C. These results are summarized in Table 2. Hexane conversions, both initial and after 5 h of time on stream, are reported for each catalyst. Li/MgO showed deactivation at almost all temperatures, however this was less significant in the case of the promoted catalysts.

The addition of 0.5 wt% MoO_3 resulted in higher initial hexane conversions than Li/MgO at almost all temperatures. This was less significant at 575 °C due to complete oxygen consumption. In addition, both at 475 and 525 °C, the catalyst exhibited higher selectivities to C_2–C_4 olefins than the unpromoted Li/MgO. Both 3.6Mo-Li and 7.1Mo-Li catalysts exhibited higher initial conversions than Li/MgO at 475 °C. However, at 525 and 575 °C these catalysts showed high activity for oxygen conversion but not for hexane. As compared to 0.5Mo-Li, catalysts with higher MoO_3 loadings, 3.6Mo-Li and 7.1Mo-Li, resulted in low selectivity to C_2–C_4 olefins. This was mainly due to formation of more of combustion products, in addition to the formation of significant amounts of C_6 products in the case of 7.1Mo-Li catalyst. Thus at all temperatures, best yields were observed with 0.5Mo-Li catalyst. 0.2Mo-Li showed almost similar initial hexane conversions as Li/MgO, however, exhibiting better stability during time on stream.

Fig. 4 shows the selectivities to different products at 575 °C for the catalysts Li/MgO, 0.5Mo-Li, 3.6Mo-Li and 7.1Mo-Li, at a similar hexane conversion of 10 mol%. Hexane conversions were maintained by varying WHSV. Both 3.6Mo-Li and 7.1Mo-Li catalysts resulted in formation of more of combustion products, while 0.5Mo-Li showed similar selectivities as Li/MgO. Significant formation of C_6 products was observed in the case of 7.1Mo-Li catalyst. The formation of C_6 products, although not clearly identified by the micro GCs, suggests the occurrence of dehydrogenation reactions in the case of 7.1Mo-Li catalyst.

In order to investigate further the role of MoO_3 on activity and to explore the ability of MoO_3 in C–H bond scission, we compared rates of hexane conversions of MoO_3-Li/MgO catalysts to those of MoO_3-MgO. Fig. 5 shows rates of hexane conversion normalized to the surface area of each catalyst. Promotion of MgO with MoO_3 did not result in any improvement in rates of hexane conversion. Moreover, in the case of Li/MgO we observed a decrease in rates of conversion with increasing MoO_3 loadings.

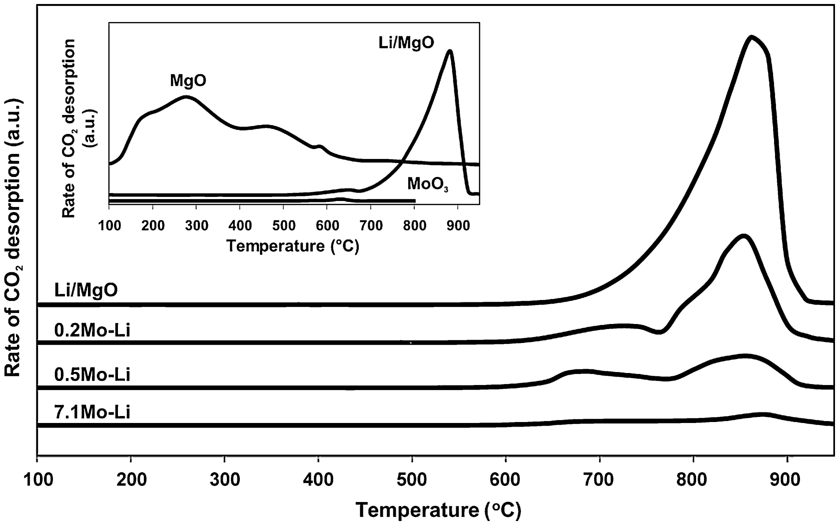

Fig. 3. Temperature programmed desorption for Li/MgO and MoO_3-Li/MgO catalysts pretreated at 600 °C (signals are normalized to the BET surface area). TPD of CO_2 for Li/MgO (100 mg), MgO (100 mg) and MoO_3 (100 mg) are included for comparison (see insert). Temperature rate 10 °C/min, He flow 10 ml/min.

Table 2
Performance of Li/MgO and MoO_3-Li/MgO catalysts during oxidative cracking of hexane (*Reaction conditions*: 100 ml/min, 10% hexane, 8% oxygen and balance He. WHSV = 15.4 h^{-1}).

	T (°C)	Conversion (mol%)			Selectivity based on C (mol%)[a]				Yields (mol%)
		C_6H_{14}		O_2	CO_x	$C_1^\circ-C_5^\circ$	$C_2^=-C_4^=$	C_6	$C_2^=-C_4^=$
		Initial	After 5 h						After 5 h
Li/MgO	475	4.26	4.19	38.80	82.47	2.80	14.77	–	0.62
	525	20.29	11.80	42.67	52.07	7.31	40.62	–	4.79
	575	40.01	28.35	65.19	24.55	14.77	60.66	–	17.20
0.2Mo-Li	475	6.36	5.60	38.82	82.77	2.45	14.78	–	0.83
	525	19.70	16.78	77.52	54.91	6.35	38.74	–	6.11
	575	40.67	39.69	99.56	28.21	12.88	58.90	–	23.38
0.5Mo-Li	475	10.72	10.65	56.04	64.17	5.43	30.40	–	3.24
	525	23.21	22.05	76.29	46.95	5.93	47.12	–	8.98
	575	40.40	38.51	99.72	28.09	11.69	60.22	–	23.19
3.6Mo-Li	475	12.12	11.17	91.70	84.38	4.17	11.45	–	1.28
	525	16.64	16.53	99.57	63.79	3.35	32.86	–	5.43
	575	24.03	23.12	99.59	47.29	6.97	45.74	–	10.57
7.1Mo-Li	475	12.51	12.02	96.42	58.96	21.58	5.42	17.18	0.65
	525	13.45	13.02	99.58	61.22	5.87	11.69	21.22	1.52
	575	20.38	19.07	99.60	48.43	6.73	24.60	20.16	4.69

[a] Selectivities after 5 h of reaction.

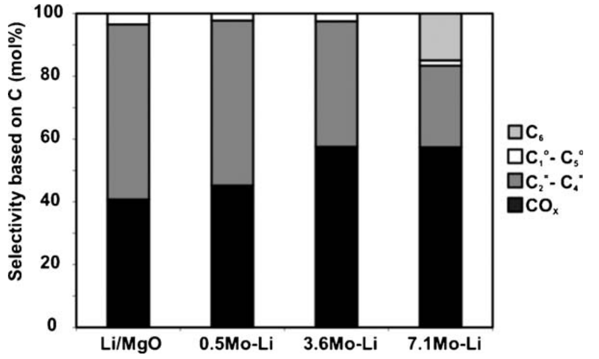

Fig. 4. Selectivity to products based on C at hexane conversion of 10 mol%. Oxygen conversions = 35 mol% (Li/MgO), 36 mol% (0.5Mo-Li), 43 mol% (3.6Mo-Li) and 53 mol% (7.1Mo-Li). *Reaction conditions*: 100 ml/min total flow, 10% hexane, 8% oxygen and He balance, *T* = 575 °C. WHSV = 154–385 h^{-1}.

4. Discussion

Oxidative cracking of hexane over Li/MgO, similar to oxidative coupling of methane [3] and oxidative dehydrogenation of lower paraffins over the same catalyst [4–8], is a heterogeneously initiated homogeneous reaction. We have proposed earlier [2] that hexane activation occurs on the catalyst surface *via* the Li^+O^- defect sites, where O^- abstracts hydrogen from a secondary carbon atom. However, we have also shown that active sites of the catalyst are susceptible for partial deactivation as result of interaction with product CO_2. We have reported earlier [2] that promotion of Li/MgO with small amounts of MoO_3 brings considerable improvement in the yield of C_2–C_4 olefins.

In order to further understand the function of MoO_3 in improving yields of olefins during the oxidative cracking of hexane, we investigated the influence of varying loadings of MoO_3 on the performance of Li/MgO. Amongst all catalysts, only 0.5Mo-Li brought considerable improvements. Li/MgO promoted with

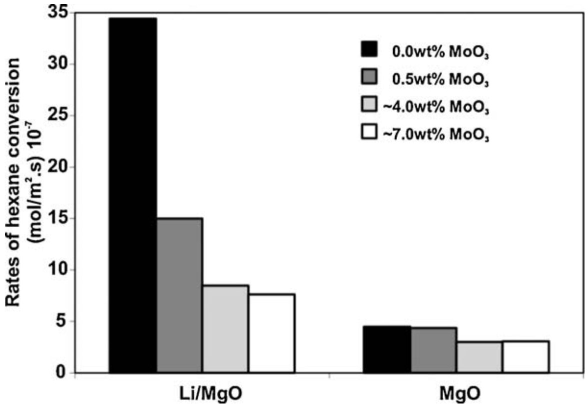

Fig. 5. Rate of hexane conversion over Li/MgO and MgO before and after promotion with varying loadings of MoO_3 (all experiments were performed in oxygen available conditions). *Reaction conditions*: 100 ml/min, 10% hexane, 8% oxygen and balance He, $T = 575\,^{\circ}C$. WHSV = 154 h^{-1}.

0.5 wt% MoO_3 exhibited higher initial hexane conversions than the unpromoted catalyst. This led to better selectivities to C_2–C_4 olefins, especially at 475 and 525 °C, mainly due to increasing the ratio of homogeneous gas phase to heterogeneous surface reactions. We reported earlier that gas phase reactions are more selective while interaction of intermediate radicals with surface O^{2-} sites of the catalyst leads to complete oxidation and CO_x formation [2]. However, increasing MoO_3 loadings, i.e. above 0.5 wt%, influenced the performance of Li/MgO negatively, as result of unselective combustion reactions which competitively consumed the oxygen in the reactant mixture, limiting hexane conversions. We have reported earlier on the significance of oxygen in increasing rates of hexane conversions [2]. In addition to combustion reactions, in the case of 7.1Mo-Li activity for dehydrogenation reactions has been as well observed. Generally, molybdenum based catalysts are extensively studied in literature for the oxidative dehydrogenation of C_2–C_4 paraffins [15–17]. Mo-MgO catalysts are reported as selective catalysts for dehydrogenation of propane and butane [18–19]. We suggest in the case of 7.1Mo-Li catalyst, the subsequent interaction of hexyl radicals with MoO_3, where the later abstracts a second hydrogen atom resulting in dehydrogenation.

Since promotion of MgO with comparable MoO_3 loadings as in Li/MgO, did not bring any considerable improvements in rates of hexane conversions (Fig. 5), we suggest that in our catalysts MoO_3 does not enhance C–H bond scission in hexane. Yoon et al. [20] reported that catalyst with excess Mo on MgO exhibited reasonable activity during oxidative dehydrogenation of propane. Similarly, Oganowski et al. [21] reported for dehydrogenation of ethylbenzene to styrene over Mo-MgO catalysts, that catalysts containing excess of MoO_3 on $MgMoO_4$ are most active. Vrieland et al. [22] reported that optimum catalyst for non-oxidative dehydrogenation of butane to butadiene consists of 15–25% of MoO_3. Most probably the MoO_3 loadings in our catalysts were too low for effective C–H bond scission in hexane.

In comparison to Li/MgO the improved initial hexane conversions with all catalysts at 475 °C, and at 525 °C with the 0.5Mo-Li catalyst (Table 2) is explained mainly by the higher surface area of the promoted catalyst. As shown in Fig. 1, Li/MgO undergoes a detrimental decrease in surface area upon calcination at temperatures above 500 °C. Since this is not observed in MgO, we believe that sintering of Li/MgO is enhanced by the presence of Li_2CO_3. Li_2CO_3 makes the catalyst susceptible for sintering at calcination temperatures above 500 °C [23]. It was reported by Trionfetti et al. [7], that during the sol–gel synthesis of Li/MgO only 40% of Li incorporates into MgO and the rest stays behind as Li_2O which interacts with ambient CO_2 to form Li_2CO_3. BET N_2 physisorption results in Table 1 show that an optimum MoO_3 loading of 0.5 wt% is sufficient to maintain high surface area upon calcination at temperatures above 500 °C. The higher surface area of the MoO_3 promoted catalyst most likely is attributed to the role of MoO_3 in minimizing these carbonates. The gradual decrease in CO_2 desorption peak area due to Li_2CO_3 with the increase in MoO_3 loadings, as observed from TPD experiments (Fig. 3), confirm the presence of less Li_2CO_3 in MoO_3 promoted catalysts. These results suggest the possible interaction of MoO_3 with Li_2CO_3. XRD (Fig. 2) of MoO_3 promoted Li/MgO showed a shift in the peak positions compared to Li/MgO, which might indicate the formation of solid solutions between MoO_3 and Li-MgO support. However, no additional peaks indicating the presence of new phases were present. Raman spectroscopy and temperature programmed techniques will be useful to identify, as function of Mo loadings, the nature of interaction of Mo with the support, thus the phases present. These studies are currently in progress.

Further as reported earlier by us [2], the significantly higher yields of olefins after longer time on stream in the case of 0.5Mo-Li catalyst is result of the better stability of the catalyst in comparison to Li/MgO. This illustrates the role of MoO_3 in minimizing the adsorption of product CO_2 during reaction on $Li^{+}O^{-}$ sites of Li/MgO, thus preventing the poisoning of the active sites.

Our results indicate that during the oxidative cracking of hexane, a minimum loading of MoO_3 (~0.5 wt%) on Li/MgO is sufficient to modify the catalyst, maintaining both higher surface area and better stability, hence leading to improved yields of C_2–C_4 olefins. Despite of the improvement of Li/MgO catalyst by promotion with MoO_3, we speculate that MoO_3 blocks some of the $Li^{+}O^{-}$ active sites in Li/MgO. This suggestion is based on the observed decrease in rates of hexane conversion normalized to surface area in the promoted catalyst as compared to the unpromoted one. This is currently under study.

5. Conclusion

The influence of varying loadings of MoO_3 on the performance of Li/MgO in oxidative cracking of hexane has been studied. Catalyst with 0.5 wt% MoO_3 loading exhibits optimal yields of C_2–C_4 olefins. This is a result of improved hexane conversions both initially as well as after time on stream, and of improved selectivities to olefins. Increasing MoO_3 loadings influences yields of olefins negatively as result of increasing combustion, as well as increasing yields of C_6 products in the case of 7 wt% MoO_3. The results also indicate that, during oxidative cracking of hexane, promotion of Li/MgO with 0.7 wt% and lower MoO_3 loadings does not enhance C–H bond scission in hexane. Apparently these loadings are too low for the catalyst to act as an effective dehydrogenation catalyst.

We conclude that promotion of Li/MgO with a minimum loading of MoO_3 of around 0.5% is sufficient to bring the following advantages; (i) minimize the amount of Li_2CO_3 originally present in Li/MgO, thus promoting the catalyst to maintain higher surface area upon calcination at 600 °C, and (ii) prevent the poisoning of the $Li^{+}O^{-}$ by product CO_2 during reaction, improving the stability of the catalyst.

Acknowledgements

The authors gratefully thank ASPECT program, the Netherlands, for financial support (project number 053.62.011). The authors also acknowledge Ing. B. Geerdink and K. Altena-Schildkamp for technical support, L. Vrielink for BET and XRF measurements, and Dr. G. Meima (Dow Benelux) for AAS measurements.

References

[1] Y. Yoshimura, N. Kijima, T. Hayakawa, K. Murata, K. Suzuki, F. Mizukami, K. Matano, T. Konishi, T. Oikawa, M. Saito, T. Shiojima, K. Shiozawa, K. Wakui, G. Sawada, K. Sato, S. Matsuo, N. Yamaoka, Catalytic cracking of naphtha to light olefins, Catal. Surv. Jpn. 4 (2) (2000) 157–167.

[2] C. Boyadjian, L. Lefferts, K. Seshan, Catalytic oxidative cracking of hexane as a route to olefins, Appl. Catal. A 372 (2010) 167–174.

[3] T. Ito, J.-X. Wang, C.-H. Lin, J.H. Lunsford, Oxidative dimerization of methane over a lithium-promoted magnesium oxide catalyst, J. Am. Chem. Soc. 107 (1985) 5062–5068.

[4] L. Leveles, K. Seshan, J.A. Lercher, L. Lefferts, Oxidative conversion of propane over lithium-promoted magnesia catalyst. II. Active site characterization and hydrocarbon activation, J. Catal. 218 (2003) 307–314.

[5] S. Fuchs, L. Leveles, K. Seshan, L. Lefferts, A. Lemonidou, J.A. Lercher, Oxidative dehydrogenation and cracking of ethane and propane over LiDyMg mixed oxides, Top. Catal. 15 (2–4) (2001) 169–174.

[6] F. Cavani, F. Trifiro, The oxidative dehydrogenation of ethane and propane as an alternative way for the production of light olefins, Catal. Today 24 (1995) 307–313.

[7] C. Trionfetti, I.V. Babich, K. Seshan, L. Lefferts, Formation of high surface area Li/MgO-efficient catalyst for the oxidative dehydrogenation/cracking of propane, Appl. Catal. A 310 (2006) 105–113.

[8] C. Trionfetti, S. Crapanzano, I.V. Babich, K. Seshan, L. Lefferts, Lithium ions incorporation in MgO for oxidative dehydrogenation/cracking of propane: active site characterization and mechanism of regeneration, Catal. Today 145 (1–2) (2009) 19–26.

[9] L. Leveles, K. Seshan, J.A. Lercher, L. Lefferts, Oxidative conversion of propane over lithium-promoted magnesia catalyst. I. Kinetics and mechanism, J. Catal. 218 (2003) 296–306.

[10] M. Xu, C. Shi, X. Yang, M.P. Rosynek, J.H. Lunsford, Effect of carbon dioxide on the activation energy for methyl radical generation over Li/MgO catalysts, J. Phys. Chem. 96 (15) (1992) 6395–6398.

[11] S.C. Bhumkar, L.L. Lobban, Diffuse reflectance infrared and transient studies of oxidative coupling of methane over Li/MgO catalyst, Ind. Eng. Chem. Res. 31 (1992) 1856–1864.

[12] J. Galuszka, Carbon dioxide chemistry during oxidative coupling of methane on a Li/MgO catalyst, Catal. Today 21 (1994) 321–331.

[13] J.L. Boldu, E. Munoz, X. Bokhimi, O. Novaro, T. Lopez, R. Gomez, Spectroscopic studies of sol–gel Li/MgO catalysts, Langmuir 15 (1999) 32–35.

[14] S.J. Korf, J.A. Roos, N.A. de Bruijn, J.G. van Ommen, J.R.H. Ross, Oxidative coupling of methane over lithium doped magnesium oxide catalysts, Catal. Today 2 (1988) 535–545.

[15] F. Cavani, N. Ballarini, A. Cericola, Oxidative dehydrogenation of ethane and propane: How far from commercial implementation? Catal. Today 127 (2007) 113–131.

[16] E. Heracleous, A.F. Lee, I.A. Vasalos, A.A. Lemonidou, Surface properties and reactivity of Al_2O_3-supported MoO_3 catalysts in ethane oxidative dehydrogenation, Catal. Lett. 88 (1–2) (2003) 47–53.

[17] J.M. Lopez Nieto, P. Botella, M.I. Vazquez, A. Dejoz, The selective oxidative dehydrogenation of ethane over hydrothermally synthesized MoVTeNb catalysts, Chem. Commun. 8 (17) (2002) 1906–1907.

[18] A. Dejoz, J.M. Lopez Nieto, F. Marquez, M.I. Vazquez, The role of molybdenum in Mo-doped V-Mg-O catalysts during the oxidative dehydrogenation of n-butane, Appl. Catal. A 180 (1999) 83–94.

[19] J.D. Pless, B.B. Bardin, H.-S. Kim, D. Ko, M.T. Smith, R.R. Hammond, P.C. Stair, K.R. Poeppelmeier, Catalytic oxidative dehydrogenation of propane over Mg-V/Mo oxides, J. Catal. 223 (2004) 419–431.

[20] Y.S. Yoon, W. Ueda, Y. Moro-oka, Oxidative dehydrogentation of propane over magnesium molybdate catalysts, Catal. Lett. 35 (1995) 57–64.

[21] W. Oganowski, J. Hanuza, B. Jezowska-Trzebiatowska, J. Wrzyszcz, Physicochemical properties and structure of $MgMoO_4$-MoO_3 catalysts, J. Catal. 39 (1975) 161.

[22] G.E. Vrieland, C.B. Murchison, Anaerobic oxidation of butane to butadiene over magnesium molybdate catalysts. I. Magnesia supported catalysts, Appl. Catal. A 134 (1996) 101–121.

[23] V. Perrichon, M.C. Durupty, Thermal stability of alkali metals deposited on oxide supports and their influence on the surface area of the support, Appl. Catal. 42 (1988) 217–227.